



U.S. DEPARTMENT OF  
**ENERGY**

Office of  
Science

DOE/SC-ARM-15-070

## **Lidar Comparison for GoAmazon 2014/15 Field Campaign Report**

HMJ Barbosa  
DA Gouveia  
B Barja  
E Landulfo

April 2016



## **DISCLAIMER**

This report was prepared as an account of work sponsored by the U.S. Government. Neither the United States nor any agency thereof, nor any of their employees, makes any warranty, express or implied, or assumes any legal liability or responsibility for the accuracy, completeness, or usefulness of any information, apparatus, product, or process disclosed, or represents that its use would not infringe privately owned rights. Reference herein to any specific commercial product, process, or service by trade name, trademark, manufacturer, or otherwise, does not necessarily constitute or imply its endorsement, recommendation, or favoring by the U.S. Government or any agency thereof. The views and opinions of authors expressed herein do not necessarily state or reflect those of the U.S. Government or any agency thereof.

# **Lidar Comparison for GoAmazon 2014/15 Field Campaign Report**

HMJ Barbosa, Universidade de São Paulo  
Principal Investigator

DA Gouveia  
B Barja  
E Landulfo  
Co-Investigators, all at Universidade de São Paulo

April 2016

Work supported by the U.S. Department of Energy,  
Office of Science, Office of Biological and Environmental Research

## **Executive Summary**

The Observations and Modeling of the Green Ocean Amazon 2014/15 (GoAmazon 2014/15) experiment uses the city of Manaus, Amazonas (AM), Brazil, in the setting of the surrounding green ocean as a natural laboratory for understanding the effects of present and future anthropogenic pollution on the aerosol and cloud life cycle in the tropics. The U.S. Department of Energy (DOE) supported this experiment through the deployment of the Atmospheric Radiation Measurement (ARM) Climate Research Facility's first Mobile Facility (AMF-1) in the city of Manacapuru, which is 100 km downwind of Manaus, from January 1 2014 to December 31 2015. During the second Intensive Operational Period (IOP) from August 15 to October 15 2014, three lidar systems were operated simultaneously at different experimental sites, and an instrument comparison campaign was carried out during the period October 4 to 10, during which the mobile lidar system from Instituto de Pesquisas Energéticas e Nucleares-Universidade de São Paulo was brought from the T2 site (Iranduba) to the other sites (T3 [Manacapuru] and then T0e-Embrapa). In this report we present the data collected by the mobile lidar system at the DOE-ARM site and compare its measurements with those from the micro-pulse lidar system running at that site.

## Acronyms and Abbreviations

AM	Amazonas (Brazilian state)
ARM	Atmospheric Radiation Measurement Climate Research Facility
AMF	ARM Mobile Facility
AN	analog mode of the lidar acquisition system
cm	centimeter
CNPq	Brazilian National Council for Scientific and Technological Development
DOE	U.S. Department of Energy
FAPESP	Fundação de Amparo a Pesquisa do Estado de São Paulo
FAPEAM	Fundação de Amparo a Pesquisa do Estado do Amazonas
GoAmazon 2014/15	Green Ocean Amazon 2014/15
Hz	hertz
INPA	Instituto Nacional de Pesquisas da Amazonia
IOP	Intensive Operational Period
IPEN	Instituto de Pesquisas Energéticas e Nucleares
IR	infrared
km	kilometer
LBA	Large Scale Biosphere Atmosphere Experiment in Amazonia
LFA	Laboratory of Atmospheric Physics
lidar	light detection and ranging
m	meter
mJ	millijoule
MPL	micro-pulse lidar
mrاد	milliradian
mW	milliwatt
nm	nanometer
PMT	photomultiplier tube
PC	photo-counting mode of the lidar acquisition system
RLS	reference lidar system
UEA	Universidade do Estado do Amazonia
USP	Universidade de São Paulo
UVRL	ultraviolet Raman lidar
VIS	visible

## Contents

Executive Summary .....	iii
Acronyms and Abbreviations .....	iv
1.0 Background.....	1
2.0 Instruments and Campaign Descriptions.....	2
3.0 Results .....	4
3.1 Signal-to-Noise Ratio.....	5
3.2 Molecular Atmosphere.....	6
3.3 Incomplete Overlap.....	7
3.4 Mixed-Phase Clouds and Polarization .....	8
3.5 Twilight Zone.....	8
3.6 Cloud Mask .....	8
4.0 Final Remarks.....	9
5.0 Lidar Comparison for GoAmazon2014/15 Presentations.....	10
6.0 References .....	10

## Figures

1. Map of the surroundings of Manaus, Brazil, showing locations of the GoAmazon2014/15 sites: T3-Manacapuru, T2-Iranduba, T1-Manaus, T0e-Embrapa, T0z-ZF2, T0a-ATTO.....	2
2. The green laser beam of the mobile Raman lidar from IPEN-USP, our reference system, taking measurements at the ARM site in Manacapuru. ....	4
3. Top panel: Logarithm of the range corrected signal (arbitrary units) for all data collected by the RLS during the campaign at the T3 site from 18:00 local time on October 5 to 11:00 local time on October 7 2014. Lower panel: MPL data for the same time period.....	5
4. Example profiles of elastic backscatter measured by UVRL-LFA and RLS-IPEN (left) on October 8, and MPL-ARM and RLS-IPEN (right) on October 6 are shown with 2- and 10-minute averages, respectively. ....	6
5. Left panel: Background and range corrected signal measures by RLS and MPL from 00:13 and 00:15 local times on October 7 2014. Right panel: The ratio of these signals, which is a good estimate of the overlap function of the MPL. ....	7
6. Cloud top (top) and base (bottom) altitudes detected by our algorithm when applied to the data set of the comparison campaign are shown in the left panel as a function of time, and in the right panel as a scatter plot.....	9

## Table

1. Basic characteristics of lidar systems operated simultaneously during GoAmazon 2014/15.....	3
--	---

## 1.0 Background

Amazonia is under continuous and constant changes, with important climatic implications (Davidson et al. 2012). The tropical forests are very important to the global hydrological cycle (Arraut et al. 2012) and to the global balance of carbon (Davidson and Artaxo 2004). Moreover, the aerosol concentration varies over a wide range, from pristine conditions to heavily polluted, following a seasonal impact of deforestation and agriculture practices (Artaxo et al. 2013). These high concentrations of aerosols play an important role in the atmospheric composition modification (Bowman et al. 2009), but also on convection, cloud formation and lifetime, and precipitation regimes (Andreae et al. 2004, Koren et al. 2012). During the wet season, the region is generally considered to be pristine; however, this condition is interrupted by occasional events of Saharan dust transport (Talbot et al. 1990) sometimes mixed with material from African biomass burning (Kaufman et al. 2005), which act as ice nuclei and contribute to increases in local convection. Last but not least, the Amazon also suffers from the impact of urban pollution. Its largest city, Manaus, is located in the central Amazon and has approximately 2 million inhabitants and 400,000 vehicles. Thermoelectric plants that emit large quantities of particulate matter, SO<sub>2</sub>, NO<sub>x</sub>, and others pollutants are still used to generate power.

The Observations and Modeling of the Green Ocean Amazon 2014/15 (GoAmazon 2014/15) experiment takes advantage of the city of Manaus in the setting of the surrounding green ocean as a natural laboratory for understanding the effects of present and future anthropogenic pollution on the aerosol and cloud life cycle in the tropics. DOE supported this experiment by deploying the AMF-1 in the city of Manacapuru, Amazonas, from January 1 2014, to December 31 2015. More information about this deployment can be found on the ARM website <http://www.arm.gov/sites/amf/mao/>, and more information about the GoAmazon 2014/15 experiment is given by Martin et al. (2015). DOE, the São Paulo State Science Foundation (FAPESP) and the Amazonas State Science Foundation (FAPEAM) also are supporting individual researchers from the United States and Brazil to extend and to use these measurements in their research (<http://www.fapesp.br/en/7792>).

During the second IOP of GoAmazon 2014/15, from August 15 to October 15 2014, three lidar systems operated simultaneously at different experimental sites as shown in Figure 1. Just before the end of IOP2, the lidar comparison campaign was carried out. The mobile lidar system was brought from the T2 site (Iranduba) to the other sites (T3 [Manacapuru] and then T0e-Embrapa) where it was operated for two days. The main objective was to use the data collected by each pair of instruments while sampling the same atmosphere to directly compare the instruments and assess their differences. This comparison should allow the correct interpretation and comparison of the physical retrievals (e.g., scattering, extinction, lidar ratio, etc.) from the three lidar systems not only during IOP2, but also during the whole GoAmazon 2014/15 experiment.

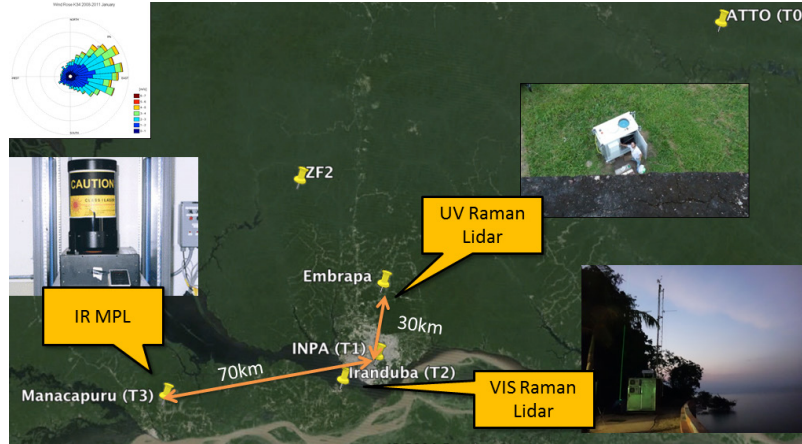


**Figure 1.** Map of the surroundings of Manaus, Brazil, showing locations of the GoAmazon2014/15 sites: T3-Manacapuru, T2-Iranduba, T1-Manaus, T0e-Embrapa, T0z-ZF2, T0a-ATTO. The photo inserts show the lidar systems at the three special sites. The wind rose on the top-left shows the prevailing wind directions in the region.

In this campaign report, we will 1) present the data collected by the mobile lidar system (hereafter called the reference lidar system or RLS) during the period of parallel measurements at the ARM Mancapuru site (October 4 to 7 2014); 2) show a direct comparison of the range and background corrected micro-pulse lidar (MPL) and RLS signals; and 3) discuss the detection of cloud base and top heights from both signals. The activities described in this report were directly funded by FAPESP (grant 13/50510-5) under the scope of one of the DOE-FAPESP-FAPEAM projects, which is coordinated by Dr. Henrique Barbosa (USP-FAPESP), who was directly involved in the measurements, Dr. Rodrigo Souza (UEA-FAPEAM), and Dr. Scot Martin (Harvard University-DOE).

Additional team members include Dr. Boris Barja, a visiting professor at the Laboratory of Atmospheric Physics (LFA) of the University of São Paulo (USP) from the Centro Meteorológico de Camaguey, Cuba, who operated the instrument at T2 and coordinated the data analysis of the three systems; Ph.D. student Diego Gouveia, from LFA-USP, who operated the RLS at T0e, T2, and T3 during the comparison campaign and participated in the data analysis; and Dr. Eduardo Landulfo, from the Center of Laser and Applications of Instituto de Pesquisas Energéticas e Nucleares-Universidade de São Paulo (IPEN-USP), who characterized/validated the RLS before its participation in GoAmazon2014/15.

We acknowledge the support from the Large Scale Biosphere Atmosphere Experiment in Amazonia (LBA), the Instituto Nacional de Pesquisas da Amazonia (INPA), and the Universidade do Estado do Amazonia (UEA). The work was conducted under 001030/2012-2 of the Brazilian National Council for Scientific and Technological Development (CNPq).

## 2.0 Instruments and Campaign Descriptions

As mentioned previously, during IOP2 from August 15 to October 15 2014, three lidar systems operated simultaneously at different experimental sites in the central Amazon region. The first system was the ultraviolet Raman lidar (UVRL) of the LFA-USP, which has been in operation since 2011 at a site 30 km upwind of Manaus (2.89°S 59.97°W), inside the Embrapa campus (Barbosa et al. 2014). Following the GoAmazon 2014/15 nomenclature, that site was designated T0e. The second was the MPL from AMF-1,



installed 80 km downwind of Manaus, in the city of Manacapuru (3.21°S, 60.59°W). This is the T3 site that was the main GoAmazon 2014/15 site where all other ARM instrumentation was installed. The third system was the mobile Raman lidar from IPEN-USP, installed 5 km downwind of Manaus, in the city of Iranduba (3.13°S, 60.13°W). This is the T2 site, which was located in front of Manaus, just across the Rio Negro. The characteristics of these systems are given in Table 1.

**Table 1.** Basic characteristics of lidar systems operated simultaneously during GoAmazon 2014/15. The lidars at T0e and T3 have been measuring continuously since the beginning of the experiment on January 1 2014, while the instrument at T2 took measurements only during IOP2.

	UV Raman Lidar LFA-USP (T0e)	VIS Raman Lidar IPEN-USP (T2)	MPL ARM AMF-1 ARM-DOE (T3)
Manufacturer	Raymetrics	Raymetrics	Sigma Space
Emission			
<i>Laser</i>	Nd-YAG	Nd-YAG	Nd-YAG, diode pumped
<i>Power</i>	95 mJ/pulse	200 mJ/pulse	10 $\mu$ J/pulse
<i>Wavelength</i>	355 nm	532 nm	532 nm
<i>Final beam width</i>	1 inch	1 inch	8 inches
<i>Repetition rate</i>	10 Hz	20 Hz	2500Hz
Detection			
<i>Field-of-view</i>	1.75 mrad	1.25 mrad	0.1 mrad
<i>Mirror</i>	40 cm	20 cm	20 cm
<i>Focal length</i>	4 m	2 m	2 m
<i>Resolution</i>	7.5 m	7.5 m	15 m
<i>Filters (FWHM)</i>	1 nm, 1nm, and 1nm	0.5 nm and 1.0 nm	0.15 nm
<i>Channels</i>	355 nm PMT <sup>a</sup> AN <sup>b</sup> PC <sup>c</sup> 387 nm PMT AN PC 408 nm PMT PC	532 nm PMT AN PC 608 nm PMT PC	532 nm avalance photodiode PC Co and Cross Pol

<sup>a</sup> PMT = photomultiplier tube  
<sup>b</sup> AN = analog mode of the lidar acquisition system  
<sup>c</sup> PC = photo-counting mode of the lidar acquisition system

The visible Raman lidar from IPEN-USP was small enough (1.2 m  $\times$  1.2 m  $\times$  80 cm) to be easily transported and hence was used as a reference for comparison against the instruments at T3 and T0e. This system is hereafter called the RLS. The other Raman system is the UVRL at T0e and is very similar to the RLS, being produced by the same company, Raymetrics, in Greece. Both use Cassengrain telescopes in a biaxial setup with Quantel CFR-400 laser with the beam expanded to 1 inch, and the detection is made using Licel Transient Recorders (TR20-160) and Hamamatsu photomultiplier tubes that can record simultaneously in analog and photon count modes, thus allowing an extended dynamical range. During IOP2, both systems were operated with 7.5 m and 30 s resolution.

The MPL deployed on AMF-1 was manufactured by Sigma Space and is a visible elastic lidar with polarization capabilities, which allows for identifying the particle shape. The system was configured for 15 m vertical and 10 s time resolutions. This system is well described by the instrument handbook (Coulter 2012) and in the literature (e.g., Campbell et al. 2002 and Flynn et al. 2007). Except for the similar telescope as used in the RLS, the components in the MPL are different in that it uses a low-power

diode-pumped laser, narrower field of view and narrower interferometric filters, polarizing beam splitters, avalanche photodiodes, and a co-axial configuration.

The comparison campaign was performed from October 4 to 7 2014, at the ARM site T3 site. On October 4, the RLS was removed from the T2 site by Dr. Barbosa and Mr. Gouveia and brought to the T3 site in a truck by the GoAmazon 2014/15 logistic coordinator, Mr. Bruno Tanaka. At the end of that day, the RLS was positioned between radiosonde and skip containers. On October 5, Mr. Gouveia arranged for an electrical power supply with help from the site ARM site manager, Mr. Vagner, and performed the optical alignment by first maximizing the signal in the far field and later verifying it using the four quadrants method. At around 18:00 local time, the RLS began making measurements (see Figure 2). In the following days, Mr. Gouveia was onsite most of the time to monitor the RLS measurements and protect the telescope from direct sunlight at local noon. At 11:00 local time on October 7, the RLS was shut down and prepared to be transported to the T0e site.



**Figure 2.** The green laser beam of the mobile Raman lidar from IPEN-USP, our reference system, taking measurements at the ARM site in Manacapuru. Photo by Rebecca Wernis.

### 3.0 Results

For the comparison campaign at the T3 site, the RLS system took measurements from around 18:00 local time on October 5 2014, to 11:00 local time on October 7 2014. Figure 3 shows the logarithm of the range corrected signal (arbitrary units) measured by the RLS (top) and MPL (bottom) for the same period with 10-minute averaging. The two panels are very similar, with the largest differences being the higher full overlap and hence lower aerosol signal in the boundary layer, and the lower signal-to-noise ratio of the

MPL at higher altitudes. In the next subsections, we discuss different aspects of the two systems, possible instrumental problems, and how they might affect the physical retrievals.

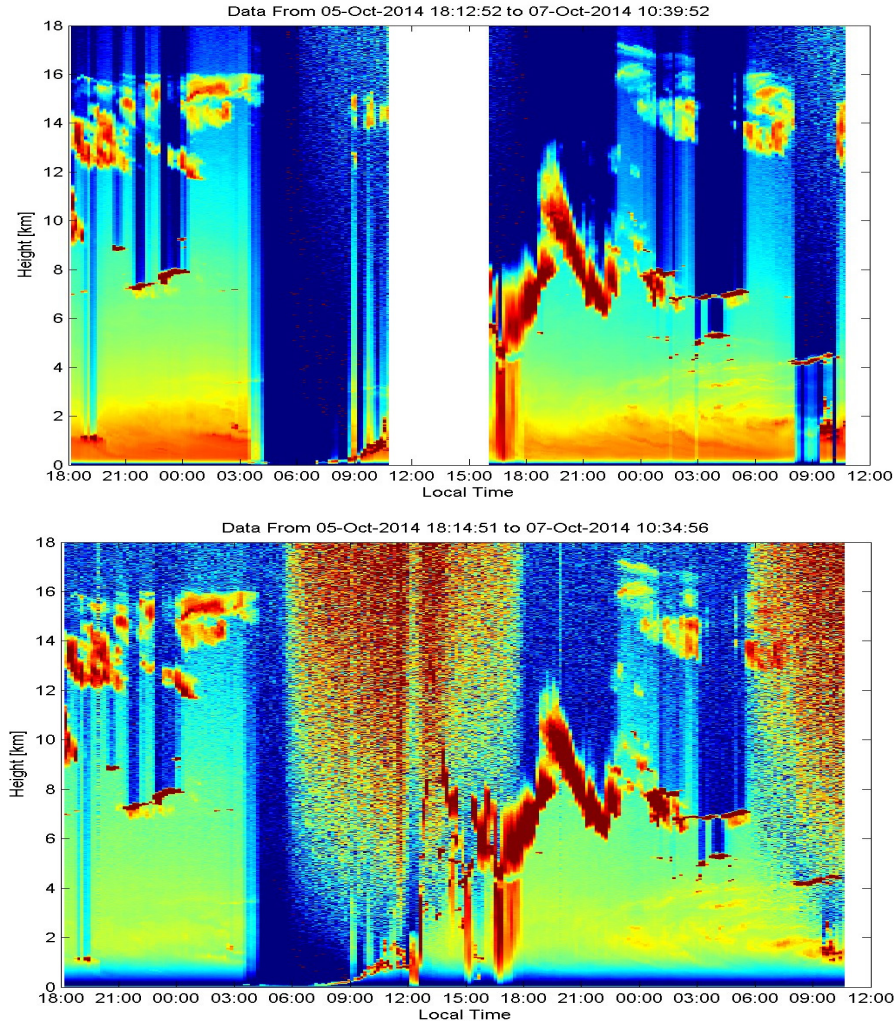


**Figure 3.** Top panel: Logarithm of the range corrected signal (arbitrary units) for all data collected by the RLS during the campaign at the T3 site from 18:00 local time on October 5 to 11:00 local time on October 7 2014. Lower panel: MPL data for the same time period. Each profile represents a 10-minute average.

### 3.1 Signal-to-Noise Ratio

The MPL uses a low-power diode-pumped laser with typically  $<25$  mW at 532 nm (eye safe), which is usually considered to be compensated by the very high repetition rates of 2500 Hz. The right panel of Figure 4, however, shows that this compensation is not enough to have similar backscatter count rates as the RLS. For the nighttime profile shown, we found a difference of about three orders of magnitude between the MPL and the RLS signals, which substantially reduce the MPL signal-to-noise ratio at typical cirrus altitude, for instance. Such a large difference is not found, for instance, when comparing the UVRL and MPL, shown in the left panel of Figure 4, for a 2-minute average profile measured by both systems side-by-side on October 8 2014 at the T0e site. Despite having a much larger mirror, the UVRL has a slower 10 Hz laser and narrower field of view, and higher molecular scattering in the ultraviolet

region reduces its signal-to-noise ratio to values slightly lower than those of the RLS, but only by a factor of 2.

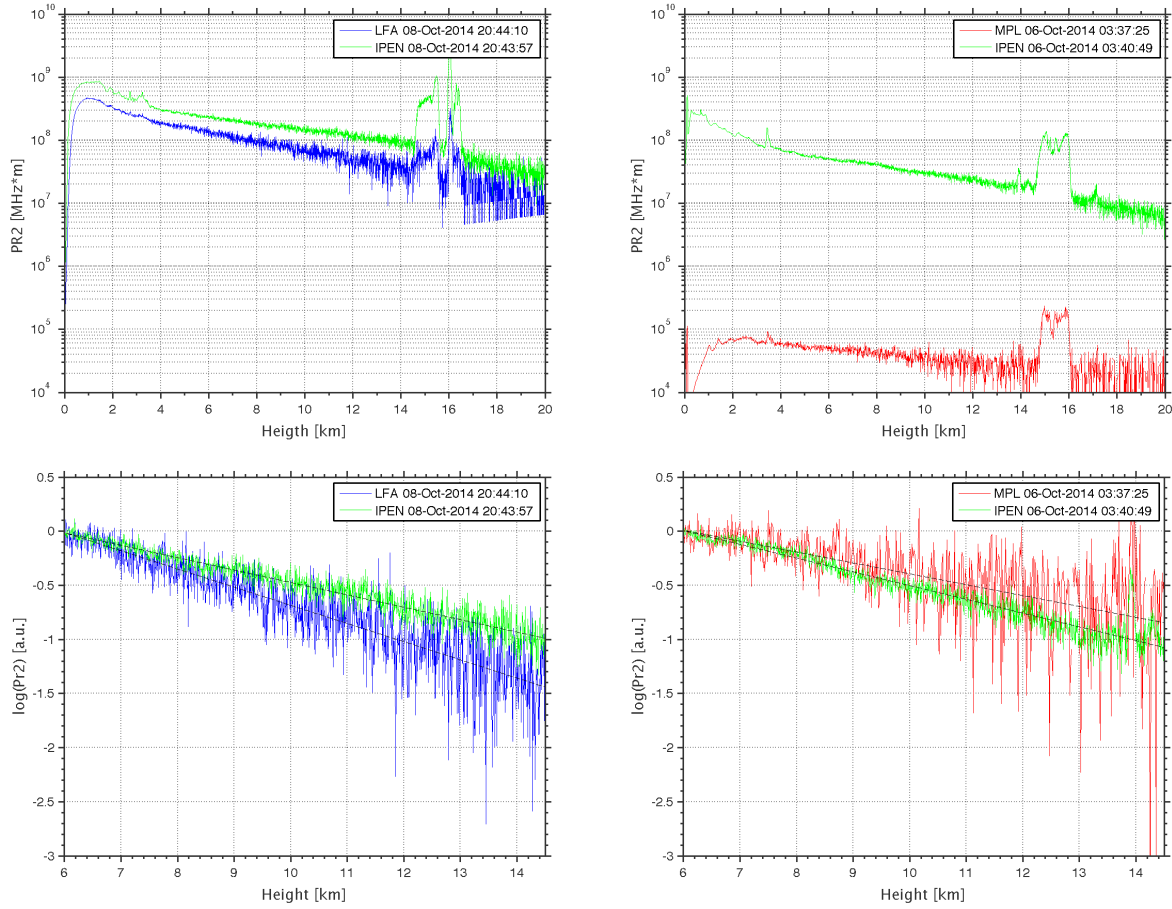


**Figure 4.** Example profiles of elastic backscatter measured by UVRL-LFA and RLS-IPEN (left) on October 8, and MPL-ARM and RLS-IPEN (right) on October 6 are shown with 2- and 10-minute averages, respectively. Top panels show the background and range corrected signals, while the lower panels show the  $\ln(Pr^2)$  normalized at 6 km. The indicated time is local time (UTC-4).

During daytime, the low signal-to-noise ratio of the MPL at higher altitudes suffers even more due to the solar background, which is clear in Figure 4. The MPL signal-to-noise ratio is so low that, even with 10-minute averages, we found it hard to use any of the daytime data above 6 km. It seems that the narrower filters and narrower field of view of the MPL are not enough to compensate the low laser power and surpass the solar background. During night time, however, the structures of the signals are similar, differing only in the near range or when a low cloud attenuates the signal. Determining whether this is a general characteristic of MPL systems or if the particular instrument at the AMF-1 has deteriorated requires further investigation.

### 3.2 Molecular Atmosphere

The upper panels of Figure 4 show examples of the range and background corrected signals for the elastic channel of the RLS and UVRL (left) and RLS and MPL (right). The boundary aerosols below 2 km

altitude can be clearly identified. The extinction coefficient of the clean molecular atmosphere (different for different wavelengths) above that 2 km can be found by the relationship  $\sigma = -0.5d\ln(Pr^2)/dr$  (i.e., using the slope method). This is indicated by the linear regression lines (dashed black lines) in the lower panels, which are showing  $\ln(Pr^2)$  normalized at 6 km. The differences between UVRL and RLS is what was expected due to the different wavelengths, but those between the RLS and MPL systems are not because they operate at the same wavelength. Whether this is an artifact of the poor signal-to-noise ratio of the 10-minute-averaged MPL profiles; or an uncorrected instrumental feature (i.e., possibly undocumented or unclear to the regular ARM MPL data user); or even an instrument issue that needs further attention will require further investigation to be determined.

### 3.3 Incomplete Overlap

Figure 5 shows a vertical range corrected signal profile simultaneously measured by the MPL and the RLS between 00:13 and 00:15 local time on October 7 2014 (2-minute average). Both signals were normalized between 10 and 14 km. Similar structures are seen in both profiles, with cirrus clouds at 7.5, 9, and 15 to 17 km, and what seems to be a plume of biomass burning aerosols just above the boundary layer up to 4 km. The near-range signals, however, are strongly affected by the incomplete overlap of the laser beam and telescope field of view: thus the measurements disagree. The MPL has full overlap expected to be at approximately 5 to 6 km (Campbell et al. 2002), while the RLS has a full overlap at approximately 200 to 300 m. Comparing the signals, however, we see good agreement only above 7 km. Therefore, we used that altitude to normalize the signals and estimated the MPL overlap function by taking the ratio 30 profiles from MPL and the corresponding profiles from the RLS. The average and standard deviation of these are shown in the right panel of Figure 5, together with the nominal overlap given in the MPL data files. There seems to be a possible misalignment of the MPL, but this needs further investigation.

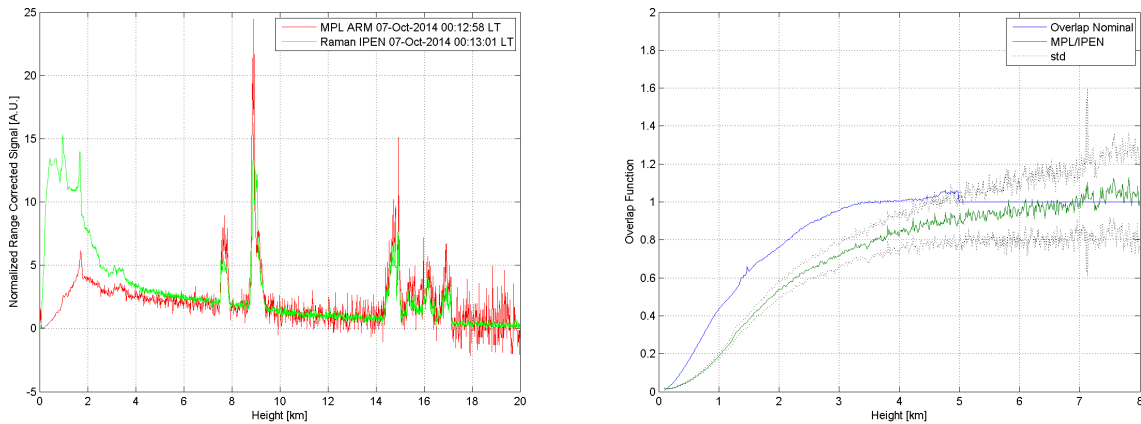


**Figure 5.** Left panel: Background and range corrected signal measures by RLS (green) and MPL (red) from 00:13 and 00:15 local times on October 7 2014. Right panel: The ratio of these signals, which is a good estimate of the overlap function of the MPL.



### 3.4 Mixed-Phase Clouds and Polarization

The case shown in Figure 5 is special because multiple layers of clouds were detected above 5 km; however, there were still good signal-to-noise ratios for both systems up to 20 km. The layers around 8 km are likely to contain both liquid water and ice, while those above 14 km must be solely made up of ice crystals. Between 6 and 7 km, 10 and 14 km, or above 18 km, the signal decreases smoothly. This indicates regions dominated by molecular scattering; thus, these layers are separated by layers of clean atmosphere. This is a very special case that can be further explored: 1) using the clean layers below and above each cloud layer to quantify the cloud scattering and extinction (e.g., using the forward and backward Klett method) and comparing this elastic MPL analysis to the Raman inversion from the RLS inelastic signal, and 2) using the MPL depolarization capability to compare the amount of depolarization in a pure ice cloud (>14 km) versus a mixed-phase cloud (7 to 10 km). This type of study could allow for a better parameterization of ice content as a function of altitude or temperature, which is important for assessing the radiative effect of such clouds, for instance.

### 3.5 Twilight Zone

During the comparison period, shown in Figure 3, various aerosol layers can be identified below 4 km and, in some cases, clouds appear exactly where the plume was located and thus should be strongly influenced by that anthropogenic contamination. This is the case at 4 km altitude, just before 09:00 local time on October 7, for instance, where there seems to be a continuous evolution from the aerosol layer into a cloud as suggested by Koren et al. (2007). This special case deserves further investigation. For instance, the MPL depolarization could be used to indicate the transition as the aerosol forms droplets, while the RLS Raman channels could be used to calculate the increased extinction as the aerosol grows. Finally, as such transitions are generally found at lower altitudes, the full MPL data set from the GoAmazon2014/5 experiment could be used to investigate this topic.

### 3.6 Cloud Mask

During the comparison period at the T3 site in Mancapuru, many types of cloud layers were measured: low cloud on top of the boundary layer, thin and thick mid-level clouds, and multi-layer cirrus clouds. Thus, it was important to evaluate if our cloud mask algorithm (Gouveia 2014) could retrieve the same cloud boundaries from data collected by the MPL and RLS instruments. The left panels of Figure 6 show the cloud base (bottom) and top (top) altitudes for the same MPL and RLS data set presented in Figure 3. The right panels show the dispersion between the measurements of the two instruments. For the cloud base altitude, there is a much better agreement than for the cloud top, as the signal is strongly scattered and not yet attenuated by the cloud itself.

From 18:00 local time on October 5 to 05:00 local time on October 6, cloud bases and tops were well captured by both systems, as clouds were optically thin and hence did not completely extinguish the laser beam. From 06:00 local time to 12:00 local time on October 6, the MPL could not detect the cirrus clouds with base at about 14 km because of the high level of noise from the sun. This is a very important finding because it means the MPL system cannot detect daytime cirrus clouds, and hence the diurnal cycle of cirrus cloud evolution cannot be directly compared at the three measurement sites of GoAmazon 2014/15. From 12:00 local time to 15:00 local time on October 6, only the MPL was operating. Despite the high noise, cloud layers below 9 km were detected but the algorithm cannot precisely define the base/top

altitudes (huge variation between consecutive profiles). From 16:00 local time to 23:00 local time on October 6, there was a thick mid-level cloud that completely attenuated the signal of both lidars. There is a good agreement for the cloud base, as expected, but the apparent cloud top by the instruments is very different. As the RLS laser is much stronger, it can penetrate further into the cloud and thus indicate a higher apparent cloud top. This is a very interesting situation that could be used to study the detection limits of the MPL.

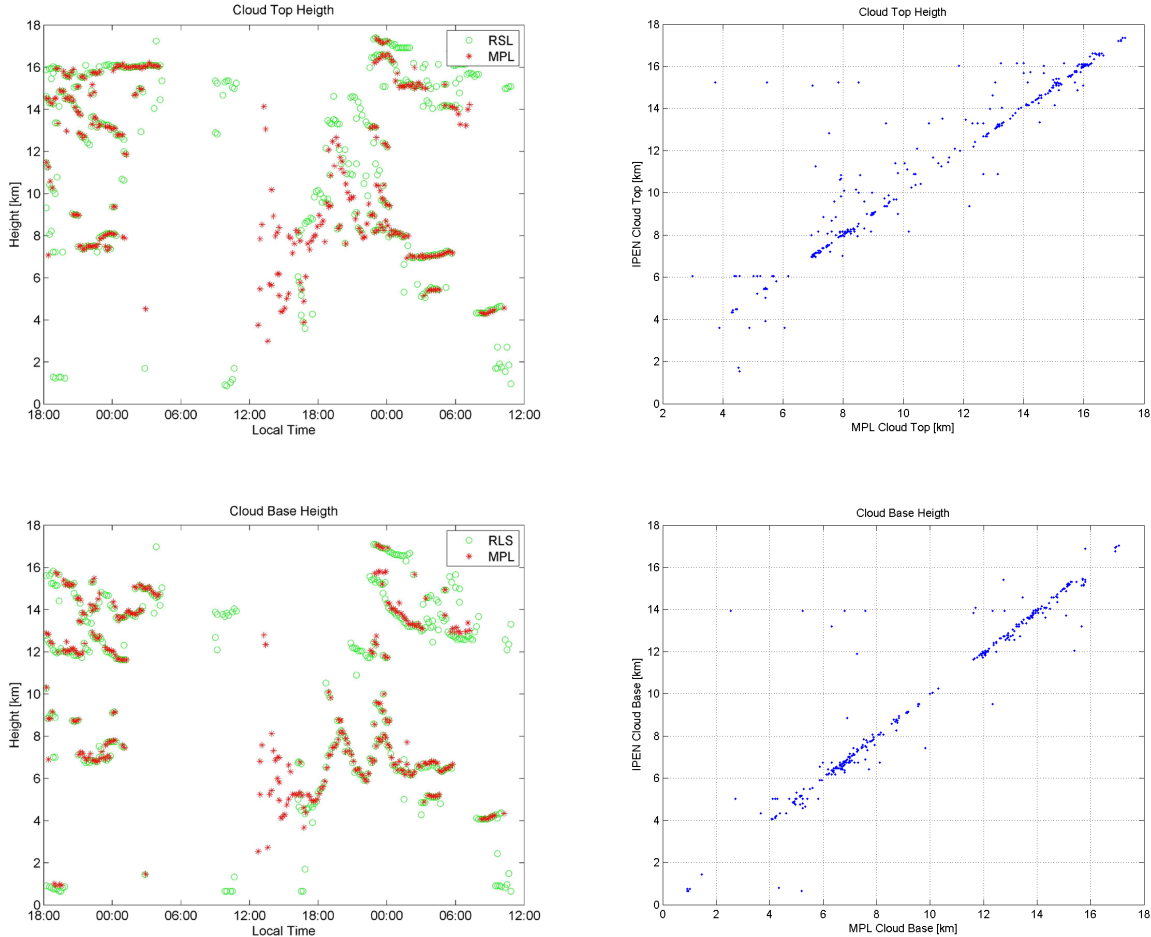


**Figure 6.** Cloud top (top) and base (bottom) altitudes detected by our algorithm when applied to the data set of the comparison campaign are shown in the left panel as a function of time, and in the right panel as a scatter plot

## 4.0 Final Remarks

The comparison campaign was very successful two reasons: 1) the efforts of all personnel involved and the valuable help of the DOE-ARM site manager and the GoAmazon2014/15 logistics manager; and 2) the excellent weather conditions experienced during those days of the dry-to-wet transition season. Although we only had parallel measurements for less than 48 hours, all possible comparison scenarios were present: single and multiple aerosol layers, some of which evolved into polluted clouds; clean atmospheric layers above and/or between the cloud layers for reference; thin mixed-phase mid-level clouds; multi-layer cirrus clouds, ranging from the typical outflow altitude of deep convection to above

the tropopause; a nocturnal halo seen by the interaction of the moonlight and the cirrus ice crystals; and a dense fog lifted with the sunrise to the top of the boundary layer, leading to rainfall quickly after. The comparison of the MPL to a reference system allowed us to identify possible instrument issues, but relevant research opportunities also were identified, as discussed throughout the report. We aim to engage in further analysis to better understand the MPL and make better use of its valuable data.

## 5.0 Lidar Comparison for GoAmazon2014/15 Presentations

Gouveia, DA, HMJ Barbosa, B Barja, P Almeida, and E Landulfo. 2015. “Intercomparison of the lidar systems operated during the GoAmazon 2014/15 experiment.” Published in Proceedings of the VIII Workshop on Lidar Measurements in Latin America, Cayo Coco, Cuba.

Gouveia, DA, HMJ Barbosa, B Barja, P Almeida, and E Landulfo. 2015. “Cirrus clouds observation and instrumental intercomparison from three lidar systems operated during IOP#2.” GoAmazon2014/15 Science Conference. Harvard University, Cambridge, Massachusetts.

## 6.0 References

Andreae, MO, D Rosenfeld, P Artaxo, AA Costa, GP Frank, KM Longo, and MAF Silva-Dias. 2004. “Smoking rain clouds over the Amazon.” *Science* 303(5662):1337-1342, [doi:10.1126/science.1092779](https://doi.org/10.1126/science.1092779).

Arraut, JM, CA Nobre, HMJ Barbosa, JA Marengo, and G Obregon. 2012. “Aerial rivers and lakes: looking at large-scale moisture transport, its relation to Amazonia and to subtropical rainfall in South America.” *Journal of Climate* 25: 543-556, [doi:10.1175/2011JCLI4189.1](https://doi.org/10.1175/2011JCLI4189.1).

Artaxo P, LV Rizzo, JF Brito, HMJ Barbosa, A Arana, ET Sena, GG Cirino, W Bastos, ST Martin, and MO Andreae. 2013. “Atmospheric aerosols in Amazonia and land use change: From natural biogenic to biomass burning conditions.” *Faraday Discussions* 165: 203-235, [doi:10.1039/c3fd00052d](https://doi.org/10.1039/c3fd00052d).

Barbosa, HMJ, B Barja, T Pauliquevis, DA Gouveia, P Artaxo, GG Cirino, RMN Santos, and AB Oliveira. 2014. “A permanent Raman lidar station in the Amazon: Description, characterization, and first results.” *Atmospheric Measurements and Techniques* 7: 1745-1762, [doi:10.5194/amt-7-1745-2014](https://doi.org/10.5194/amt-7-1745-2014).

Bowman, DMJS, JK Balch, P Artaxo, WJ Bond, JM Carlson, MA Cochrane, CM D’Antonio, RS DeFries, JC Doyle, SP Harrison, FH Johnston, JE Keeley, MA Krawchuk, CA Kull, JB Marston, MA Moritz, IC Prentice, CI Roos, AC Scott, TW Swetnam, GR van der Werf, and SJ Pyne. 2009. “Fire in the earth system.” *Science* 324(5926): 481-484, [doi:10.1126/science.1163886](https://doi.org/10.1126/science.1163886).

Campbell, JR, DL Hlavka, EJ Welton, CJ Flynn, DD Turner, JD Spinhirne, VS Scott III, and IH Hwang. 2002. “Full-time, eye-safe cloud and aerosol lidar observation at Atmospheric Radiation Measurement program sites: Instruments and data processing.” *Journal of Atmospheric and Oceanic Technology* 19: 431-442, [doi:10.1175/1520-0426\(2002\)019<0431:FTESCA>2.0.CO;2](https://doi.org/10.1175/1520-0426(2002)019<0431:FTESCA>2.0.CO;2).

Coulter, R. 2012. *Micropulse Lidar (MPL) Handbook*. Technical Report DOE/SC-ARM/TR-019 available at ARM website: [https://www.arm.gov/publications/tech\\_reports/handbooks/mpl\\_handbook.pdf](https://www.arm.gov/publications/tech_reports/handbooks/mpl_handbook.pdf).



Davidson, EA, and P Artaxo. 2004. “Globally significant changes in biological processes of the Amazon Basin: results of the Large-Scale Biosphere-Atmosphere Experiment.” *Global Change Biology* 10(5): 519-529, [doi:10.1111/j.1529-8817.2003.00779.x](https://doi.org/10.1111/j.1529-8817.2003.00779.x).

Davidson, EA, AC Araújo, P Artaxo, JK Balch, IF Brown, MMC Bustamante, MT Coe, RS DeFries, M Keller, M Longo, W Munger, W Schroeder, BS Soares-Filho, CM Souza, and SC Wofsy. 2012. “The Amazon Basin in transition.” *Nature* 481(7381): 321-328, [doi:10.1038/nature10717](https://doi.org/10.1038/nature10717).

Flynn, CJ, A Mendoza, Y Zheng, and S Mathur. 2007. Novel polarization-sensitive micropulse lidar measurement technique.” *Optics Express* 15 (6): 2785-2790, doi:[10.1364/OE.15.002785](https://doi.org/10.1364/OE.15.002785).

Gouveia, DA. 2014. *Caracterização de Nuvens Cirrus na Região da Amazônia Central Utilizando um LIDAR em Solo*. In Portuguese, Master of Science Dissertation, Instituto de Física-Universidade de São Paulo. Abstract in English available at <http://www.teses.usp.br/teses/disponiveis/43/43134/tde-29092014-120815/fr.php>.

Kaufman, YJ, I Koren, LA Remer, D Tanré, P Ginoux, and S Fan. 2005. “Dust transport and deposition observed from the Terra-Moderate Resolution Imaging Spectroradiometer (MODIS) spacecraft over the Atlantic Ocean.” *Journal of Geophysical Research* 110: D10S12, [doi:10.1029/2003JD004436](https://doi.org/10.1029/2003JD004436).

Koren, I, LA Remer, YJ Kaufman, Y Rudich, and JV Martins. 2007. “On the twilight zone between clouds and aerosols.” *Geophysical Research Letters* 34(8): L08805, [doi:10.1029/2007GL029253](https://doi.org/10.1029/2007GL029253).

Koren, I, O Altaratz, LA Remer, G Feingold, JV Martins, and RH Heiblum. 2012. “Aerosol-induced intensification of rain from the tropics to mid-latitudes.” *Nature Geoscience* 5: 118-122, [doi:10.1038/ngeo1364](https://doi.org/10.1038/ngeo1364).

Martin, ST, P Artaxo, LAT Machado, AO Manzi, RAF Souza, C Schumacher, J Wang, MO Andreae, HMJ Barbosa, J Fan, G Fisch, AH Goldstein, A Guenther, JL Jimenez, U Pöschl, MA Silva Dias, JN Smith, and M Wendisch. 2015. “Introduction: Observations and modeling of the Green Ocean Amazon (GoAmazon2014/5).” *Atmospheric Chemistry and Physics* 15: 30175-30210, [doi:10.5194/acpd-15-30175-2015](https://doi.org/10.5194/acpd-15-30175-2015).

Talbot, RW, MO Andreae, H Berresheim, P Artaxo, M Garstang, RC Harriss, KM Beecher, and AM Li. 1990. “Aerosol chemistry during the wet season in Central Amazonia: The influence of long-range transport.” *Journal of Geophysical Research* 95(D10): 16955-16969, [doi:10.1029/JD095iD10p16955](https://doi.org/10.1029/JD095iD10p16955).



U.S. DEPARTMENT OF  
**ENERGY**

---

Office of Science